Linkage Isomerization as a Mechanism for Photochromic Materials: Cyclopentadienylmanganese Tricarbonyl Derivatives with Chelatable Functional Groups

Tung T. To,[†,⊥] Charles B. Duke III,[†] Christopher S. Junker,[†] Casey M. O'Brien,[†] Charles R. Ross II,[‡] Craig E. Barnes,[#] Charles Edwin Webster,[†] and Theodore J. Burkey*[,†]

Department of Chemistry, The University of Memphis, Memphis, Tennessee 38152-3550, Department of Chemistry, University of Tennessee, Knoxville, Tennessee, 37996-1600, and Department of Structural Biology, St. Jude Children's Research Hospital, MS 311, 332 N. Lauderdale, Memphis, Tennessee 38105-2794

Received October 31, 2007

Two, bifunctional side-chain cyclopentadienylmanganese tricarbonyl complexes, **7** (pyridine and ketone side chain) and **14** (thioamide and pyridine side chain), were prepared and converted to chelates following CO dissociation by UV irradiation. Both pyridine (**8**) and carbonyl (**9**) chelates are observed following irradiation of **7**. In contrast, only thioamide chelate (**16**) is observed following irradiation of **14** even though a pyridine group was available. Visible irradiation isomerizes the pyridine chelate **8** to the carbonyl chelate **9**, which thermally isomerizes back to **8** at 25 °C in a few minutes, demonstrating a photochromic response from a cyclopentadienyl-manganese complex based on a linkage isomerization of a tethered functional group. DFT calculations predicted that the activation enthalpy of thermal linkage isomerization would be 20.8 kcal/mol and that the mechanism is likely an associative process that does not involve a simple dissociation of the manganese bond to the side-chain ketone. The DFT calculations were supported by subsequent dynamic NMR experiments that yielded an activation enthalpy and entropy of 21.4 ± 0.8 kcal/mol and 3.5 ± 0.1 eu, respectively. The studies indicate that a compound with a tethered, coordinated functional group, which is otherwise not labile, can isomerize by a low-energy pathway if there is an appropriate "conduit" to another functional group with a stronger metal–ligand bond. Thus, the preparation of photochromic organometallic complexes based on linkage isomerization will require a bridge that inhibits an associative walk between functional groups if they are to be bistable.

Introduction

There has been substantial development of organic photochromic systems,[1] but comparatively little research on organometallic systems.[2,3] We are developing photochromic systems that are efficient, reversible, metal-ligand photosubstitutions for use in molecular devices. To minimize fatigue, ultrafast substitutions with high quantum yields are desirable. Our studies of chelation following ligand photodissociation have revealed the first examples of unit quantum yields for organometallic photosubstitution.[4] These studies led to the design of compounds that undergo ultrafast chelation while eliminating competing ultrafast reactions (such as solvent coordination) that otherwise could lower quantum yields.[5] The solvent can have a dramatic and divergent effect on the distributions of ultrafast products. We observed in heptane that analogous manganese and chromium complexes behave similarly, exhibiting competing chelation and solvent coordination; but in acetonitrile, chelation occurs exclusively for the manganese complexes, while solvation occurs exclusively for the chromium complexes.[6]

Another objective was to couple the motion of two functional groups such that the dissociation of one group initiates the addition of the other group. We recently reported several $Cp(Mn(CO)_2L)$ that are photochromic via a linkage isomerization, where L is a bifunctional but not a chelatable ligand.[2] All the complexes showed fatigue in their photochromic response. An example is the photochromic pair **1/2** (Scheme 1), where the occasional cage escape of the ligand leads to side reactions. The mechanisms for side reactions most likely involve the formation of solvated intermediates, which provide an opportunity for the ligand to escape the solvent cage.[2] Tethering the two functional groups to the metal would keep them in the solvent cage and allow the formation of two spectroscopically different chelates, although the stability of the chelates and the yields for linkage isomerization are likely to depend on the

* Corresponding author. E-mail: tburkey@memphis.edu.
† The University of Memphis.
# University of Tennessee.
‡ St. Jude Children's Research Hospital.
⊥ Current address: Physics Laboratory, National Institute of Standards and Technology, 100 Bureau Drive, Stop 8443, Gaithersburg, Maryland 20899.

(1) Irie, M. Ed. Photochromism: Memories and Switches. *Chem. Rev.* **2000**, *100*, 1683–1890.
(2) To, T. T.; Barnes, C. E.; Burkey, T. J. *Organometallics* **2004**, *23*, 2708–2714.
(3) For recent studies and leading references: Rachford, A. A.; Rack, J. J. *J. Am. Chem. Soc.* **2006**, 14318–14324.
(4) Pang, Z.; Burkey, T. J.; Johnston, R. F. *Organometallics* **1997**, *16*, 120–123.
(5) (a) Jiao, T.; Pang, Z.; Burkey, T. J.; Johnston, R. F.; Heimer, T. A.; Kleinman, V. D.; Heilweil, E. J. *J. Am. Chem. Soc.* **1999**, *121*, 4618–4624. (b) Yeston, J. S.; To, T. T.; Burkey, T. J.; Heilweil, E. J. *J. Phys. Chem. B* **2004**, *108*, 4582–4585. (c) To, T. T.; Heilweil, E. J.; Burkey, T. J. *J. Phys. Chem. A* **2006**, *110*, 10669–10673.
(6) To, T. T.; Heilweil, E. J.; Duke, C. B., III; Burkey, T. J. *J. Phys. Chem. A* **2007**, *111*, 6933–6937.

10.1021/om701101h CCC: $40.75
Publication on Web 01/03/2008

Scheme 1

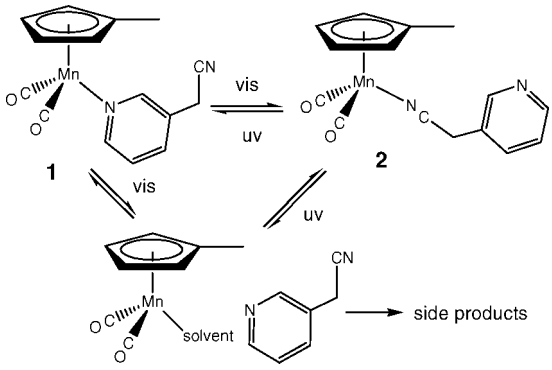

Scheme 2

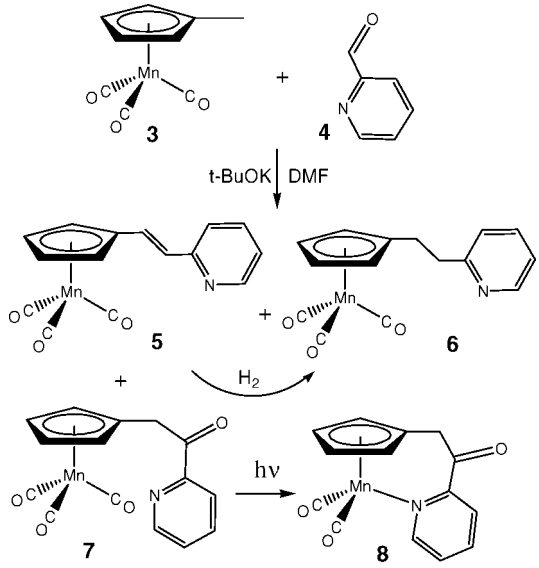

structure of the tether and the functional groups. In the current study, two cymantrene derivatives with bifunctional side chains have been prepared and their photochemical reactions have been characterized. One derivative has tethered pyridine and carbonyl groups, and the other has tethered pyridine and thioamide groups. The chelates formed following photolysis are photochromic in the first case but not in the second.

Results and Discussion

Tethered Pyridine and Carbonyl Groups. We prepared **8** and investigated its photochromic response, which is based on the linkage isomerization between the pyridine and carbonyl groups. Interpretation of the results is facilitated by a comparison with **16**, a compound with tethered pyridine and thioamide groups (Scheme 6) that shows properties similar to **8** but is not photochromic.

The preparation of **7**, the precursor of **8**, was adapted from a Siegrist alkene synthesis[7] and produced the alkene elimination product **5** with a low yield of **7** (3%) (Scheme 2). Based on the assumption that **7** was formed via a mechanism analogous to that for the Meerwein−Ponndorf−Verley reaction, the conditions were optimized to obtain **7** in 34% yield (no **5** and 17% **6**, Table S1, Supporting Information). Four Cp and four pyridine

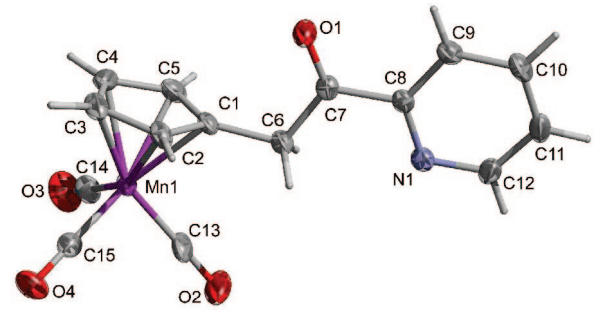

Figure 1. ORTEP of **7** with 50% anisotropic displacement ellipsoids. Selected bond lengths (Å), angles (deg), and torsion angles (deg) for **7**: C1−Mn1: 2.153(3); C6−C1−Mn1: 126.7(2); C1−C6−C7: 112.2(3); C6−C7−C8: 117.2(3); N1−C8−C7: 116.9(3); C13−Mn−C14: 90.50(16); O1−C7−C8−N1: –178.1(3).

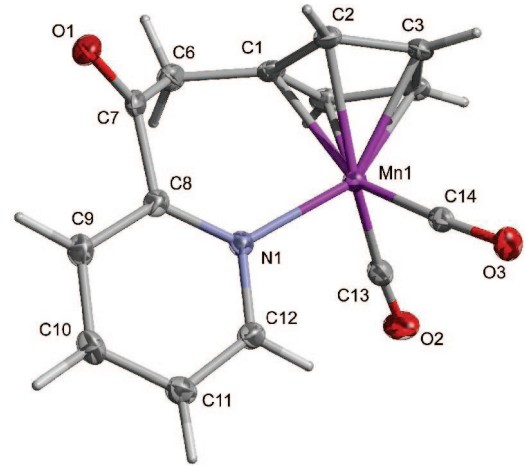

Figure 2. ORTEP of **8** with 50% anisotropic displacement ellipsoids. Selected bond lengths (Å), angles (deg), and torsion angles (deg) for **8**: Mn1−N1: 2.0666(14); C1−Mn1: 2.1435(15); C6−C1−Mn1: 120.94(10); C1−C6−C7: 109.00(14); C6−C7−C8: 118.33(14); N1−C8−C7: 121.10(15); C13−Mn1−C14: 89.77(7); C13−Mn1−N1−C12: 44.55(13); C14−Mn1−N1−C12: –45.71(12); C11−C12−N1−Mn1; 172.68(13); O1−C7−C8−N1: –143.06(16).

protons were observed in the proton NMR spectra for **5**, **6**, and **7**; however, **7** was distinguished from **5** and **6** by a singlet methylene proton peak (2H, 4.23 ppm) and ketone carbon peak (197.3 ppm), while **5** had coupled vinyl peaks (1H, 6.82 and 1H, 7.13 ppm) and **6** had coupled methylene peaks (2H, 2.72 ppm and 2H, 2.96 ppm). The structure of **7** was further confirmed by X-ray crystallography (Figure 1 and Supporting Information). Finally, **7** is synthetically related to **8** via chelation of the pyridine ring following photolysis of **7** (Scheme 2), and the structure of **8** was also confirmed by X-ray crystallography (Figure 2 and Supporting Information). Dilute solutions of **7** were typically colorless to light yellow, while those for **8** were dark purple to black; thus **7** and **8** are distinguished by their large difference in the lowest optical transition ($\epsilon_{330} = 1800\ M^{-1}\ cm^{-1}$ versus $\epsilon_{482} = 920\ M^{-1}\ cm^{-1}$ in benzene, respectively). These results are consistent with the observed red shifts following CO substitution of $CpMn(CO)_3$ by pyridine derivatives.[2,8]

A photochromic response was demonstrated by changes in UV–vis, NMR, and IR spectra following irradiation of **8** (Scheme 3). A purple heptane solution of **8** has peaks at 425

(7) (Tricarbonyl)[{2-(4-methoxyphenyl)ethenyl}-5-cyclopentadienyl]-manganese from **3** and *N*-[(4-methoxyphenyl)methylene]benzenamine:(a) Eberhardt, R.; Schloegl, K. *Syn. React. Inorg. Metal-Org. Chem.* **1974**, *4*, 317–323. (b) Siegrist, A. E.; Meyer, H. R.; Gassmann, P.; Moss, S. *Helv. Chim. Acta* **1980**, *63*, 1311–1334.

(8) Giordano, P. J.; Wrighton, M. S. *Inorg. Chem.* **1977**, *16*, 160–166.

Scheme 3

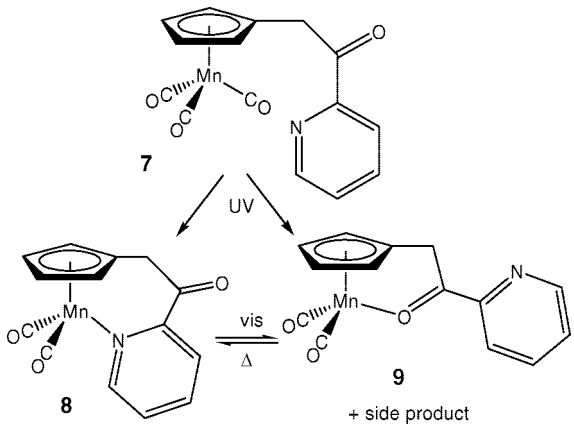

and 572 nm that decay during visible irradiation as the solution turns blue, and a shoulder grows at 750 nm with an isosbestic point at 584 nm (Figure 3). After irradiation ceases, the 750 nm shoulder decays away as the solution returns to purple in less than 10 min in the dark, but a new isosbestic point at 578 nm is observed during the decay, and the absorbance at 572 nm decreased by 3%, indicating the formation of side product. Difference spectra reveal a peak at 680 nm during UV irradiation corresponding to a transient photoproduct assigned to the structure of **9** (see Figure S1, Supporting Information).

IR spectral changes upon visible irradiation of **8** are shown in Figure 4. Peaks assigned to **8** at 1941 and 1878 cm^{-1} decrease upon visible irradiation and overlap with two IR peaks that grow

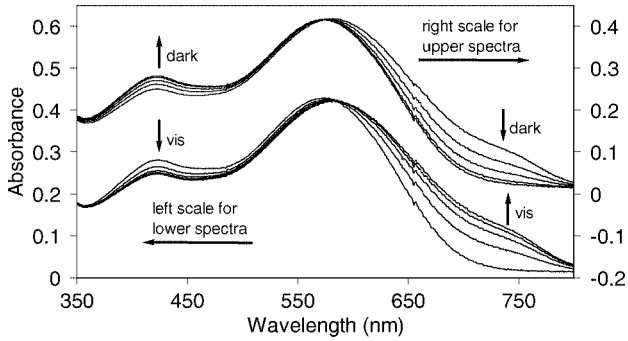

Figure 3. UV–vis spectra of 62 μM **8** in heptane at room temperature during visible irradiation (lower spectra) and subsequent dark reaction (upper spectra). Lower spectra were recorded after a total of 0, 20, 40, 60, and 80 s of irradiation. Without further irradiation, upper spectra were recorded at additional 0, 40, 120, 240, and 360 s.

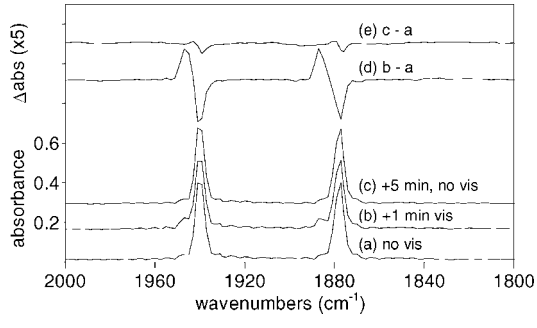

Figure 4. IR spectral changes for 0.61 mM **8** in heptane: (a) before visible irradiation, (b) after 1 min of visible irradiation, (c) after additional 5 min without irradiation, (d) difference spectra from b to a, and (e) difference spectra from c to a.

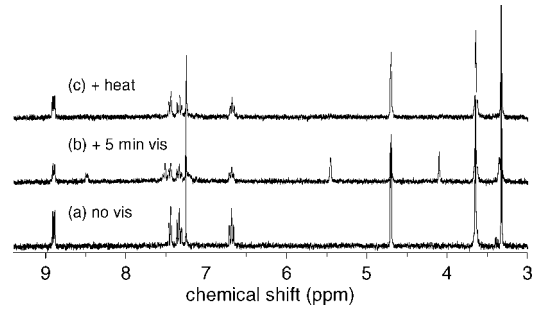

Figure 5. ^{1}H NMR spectra of 10 mM **8** at 5 °C in methylcyclohexane-d_{14}: (a) no irradiation, (b) after 5 min visible irradiation at –25 to –5 °C, and (c) subsequent warming to 25 °C and returning to 5 °C.

at 1947 and 1887 cm^{-1}. The latter peaks assigned to **9** are most easily detected in difference spectra (before and after irradiation), where positive peaks correspond to new peaks and negative peaks to loss of starting compound. After 5 min at room temperature, the new peaks decrease as the original peaks increase but without complete recovery, as indicated by the lack of a flat baseline in the final difference spectra. This also indicates small amounts of side product are forming.

Similar experiments revealed that NMR peaks assigned to **8** decreased during 5 min visible irradiation of **8** at 5 °C in methylcyclohexane-d_{14} while new peaks appeared and the solution turned blue (Figure 5, see Table 1 for assignments). Thus, the NMR peaks that appear with the blue chromophore are assigned to **9**. When the sample was allowed to warm to 25 °C without further irradiation, the peaks assigned to **8** grew while those for **9** disappeared. The area ratio of the pyridine *ortho* hydrogens for **9** at 8.46 ppm and **8** at 8.87 ppm indicated a 25% conversion to **9**.

The coordination of a ketone carbonyl group in **9** to our knowledge has not been reported previously for cyclopentadienyl manganese complexes. For comparison, a pale yellow solution of **3** and acetophenone in benzene-d_6 changed to dark red during 1 min UV irradiation, and the proton NMR spectrum had two new Cp peaks at 4.19 and 4.49 ppm, indicating at least 16% conversion to a product. The dark red solution faded as the new NMR peaks decayed away and the NMR peaks of **3** recovered in 15 min. This suggests that the kinetic stability of a coordinated acetophenone carbonyl complex is about the same as that observed for **9** since the coordination of a benzene ring is not observed under similar conditions.[2]

The results of Figures 3–5 clearly demonstrate that **8** and **9** constitute a photochromic system: visible irradiation leads to a color change during linkage isomerization of **8** to **9** followed by a reverse color change during a thermal linkage isomerization back to **8**. Inspection of difference UV–vis spectra (Figure S1, Supporting Information) suggests that at low temperature (barring side-product formation) the system might be driven to **8** by irradiating at 750 nm or to **9** by irradiating at 430 nm. The system is not completely reversible, and at least one other product is formed besides **8** and **9** as noted above.

Kinetics of Linkage Isomerization. The mechanism of isomerization of **9** to **8** was first investigated computationally (Scheme 4). The lowest energy isomerization pathway from **9** to **8** proceeds via three steps: **9** (the lower energy oxygen-bound linkage isomer with a carbonyl to pyridine *s-trans* conformation) to **19** (an η^2 π-bound carbonyl intermediate), **19** to **18** (an η^2 π-bound pyridyl intermediate), and **18** to **8** (the nitrogen-bound linkage isomer). The computed activation enthalpy is 20.8 kcal/mol (**9** to TS-**18**−**19**). Computed geometric parameters for

Table 1. ^{1}H NMR Resonances of Cymantrene Derivatives and the Chelates (ppm)[a]

	CH_2	CH	3,4-Cp	2,5-Cp	3-py	4-py	5-py	6-py	CH_3/NH_2
7	4.23		4.91	5.10	8.06	8.08	7.72	8.79	
7[b]	4.14		4.50	4.76	7.68	8.02	7.31	8.61	
8	3.52		3.85	5.00	7.51	7.81	7.21	8.80	
8[b]	3.30		3.62	4.67	7.43	7.61	6.66	8.87	
9[b]	3.33		4.08	5.43	7.48	7.50	7.19	8.46	
12	2.92	4.60	4.93	4.93	7.43	7.85	7.41	8.60	
14	3.04	4.24	4.88	4.88	7.46	7.75	7.28	8.51	9.5,9.6
15	2.4, 2.9	4.5	3.6, 3.9	5.1, 5.3	7.62	7.81	7.10	9.11	
16	2.4, 3.2	4.3	3.4, 3.8	4.1, 4.6	7.33	7.80	7.31	8.63	9.2, 10.5
17	2.4,2.8	4.15	3.3, 3.9	4.9, 5.3	7.65	7.78	6.98	9.10	9.5, 10.0

[a] Dimethylsulfoxide-d_6 except where noted. [b] Methylcyclohexane-d_{16}, 5 °C.

Scheme 4. Diagrammatic representation of the computed structures involved in the isomerization of 9 to 8. Energies are given in kcal/mol relative to 8

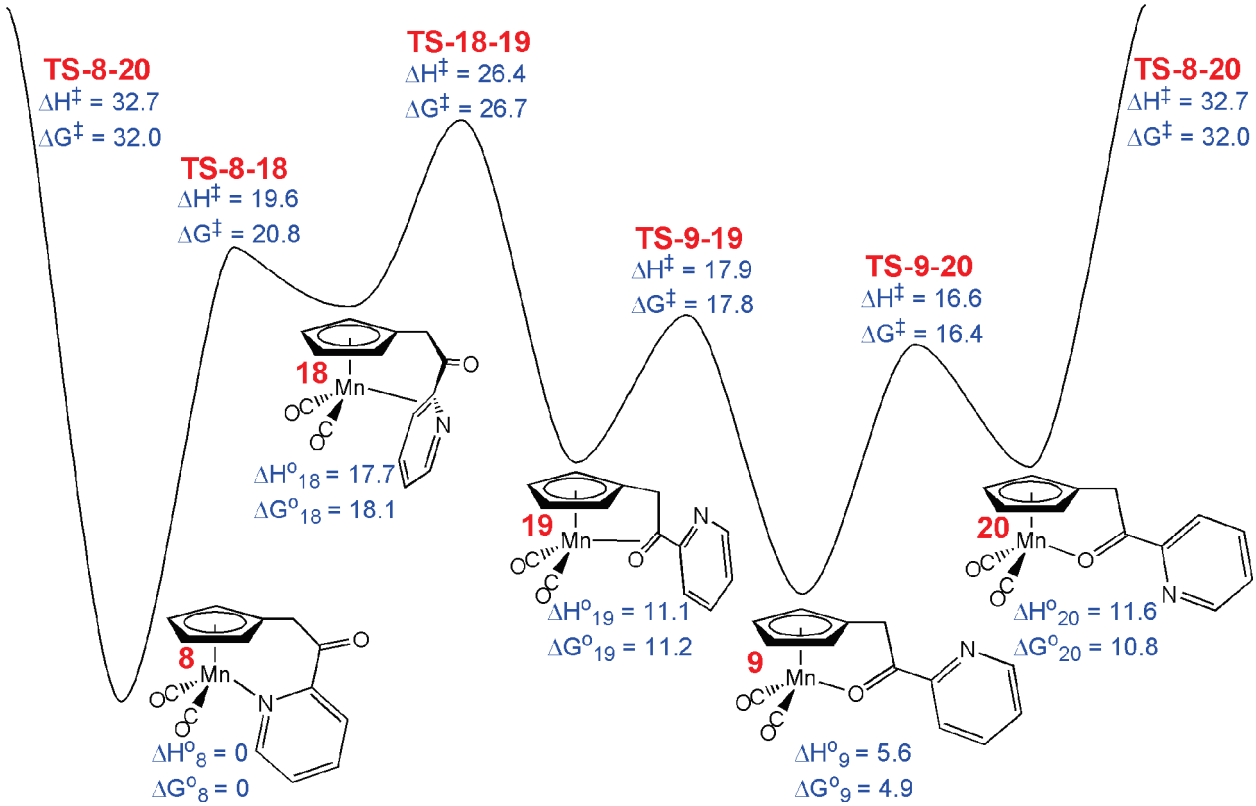

optimized geometries of **8**, **9**, **18**, and **19** are given in Figure 6. Confirmation of the calculations was obtained from kinetic experiments where the rates of decay of proton NMR peaks for **9** and the recovery of those for **8** were found to be equal and first-order in **9** (Figure 7, and Table S4, Supporting Information). The experimental activation enthalpies obtained from the Eyring plots (Figure 8, 22.0 ± 0.5 and 20.8 ± 0.2 kcal/mol, respectively) were in good agreement with the computed activation enthalpy. Furthermore, the computational $\Delta H^{\ddagger}$ and $\Delta G^{\ddagger}$ are very similar in value, indicating that $T\Delta S^{\ddagger}$ is small (−1.0 kcal/mol at 25 °C). This value is also in good agreement with the small *experimental* $T\Delta S^{\ddagger}$ (1.0 kcal/mol), which was obtained from the experimental activation entropy of 3.5 ± 0.1 eu (calculated using the average experimental activation enthalpy of 21.4 ± 0.8 kcal/mol). A low activation entropy is consistent with a pathway where the side chain never dissociates from the metal as proposed for **9** → **19** → **18** → **8**. The computational results for intermediates **19** with a η^2 metal–carbonyl interaction and likewise **18** with a η^2 metal−pyridine interaction (that does not involve the nitrogen) suggest a mechanism where the metal walks along the π-bonds of the side chain from one functional group to another instead of complete dissociation from the side chain followed by addition of the pyridyl group. An η^2-arene to η^1-N linkage isomerization has been reported for other complexes.[9] Additional computational results indicate that dissociation of the side-chain functional group to form a coordinatively unsaturated 16-electron complex followed by rotation and coordination by the second functional group (dissociation pathway **9**−**21**−**22**−**8**, Schemes S1 and S4, Supporting Information) is higher in energy than the π-bound pathway. A two-step pathway from **9** to **8** was also found: **9** to **20** (the higher energy *s-cis* conformer of the oxygen-bound linkage isomer) and **20** to **8**. However, this two-step pathway (**9**−**20**−**8**) is higher in energy by more than 6 kcal/mol compared to the π-bound pathway (Scheme 4).[10,11]

Tethered Pyridine and Thioamide Groups. The bifunctional derivative **14** was prepared by way of **12**. Lithiation of 2-cyanomethylpyridine followed by alkylation with **11** gave a reasonable yield of **12** as well as substantial formation of **13**

(9) For recent work see: Delafuente, D. A.; Kosturko, G. W.; Graham, P. M.; Harman, W. H.; Myers, W. H.; Surendranath, Y.; Klet, R. C.; Welch, K. D.; Trindle, C. O.; Sabat, M.; Harman, W. D. *J. Am. Chem. Soc.* **2007**, *129*, 409–416.

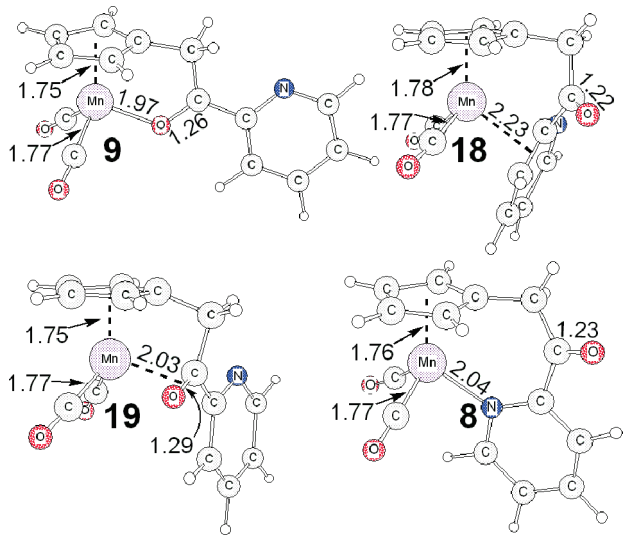

Figure 6. Optimized structures of **8**, **9**, **18**, and **19**. Distances are given in Å.

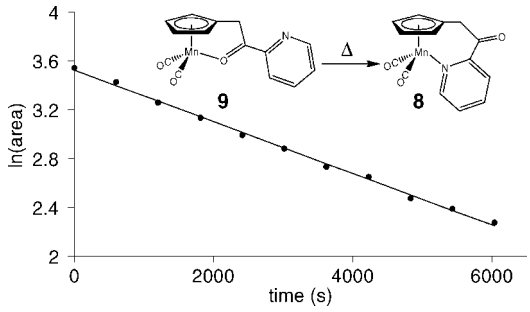

Figure 7. Decay of NMR peak area at 5.43 ppm for **9** following photolysis of μM **7** in methylcyclohexane-d_{14} at 272.4 K.

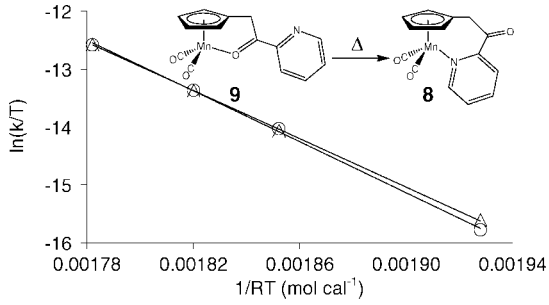

Figure 8. Eyring plots for decay of **9** (triangles) and formation of **8** (circles) in methylcyclohexane-d_{14}.

(Scheme 5). **12** is readily distinguished from **13** by the presence of a methine proton (Table 1) and its lower area of Cp versus pyridine peaks. **13** was further identified by its crystal structure. The assignment of a metal tricarbonyl structure for **12** is consistent with the absence of an absorption band longer than 400 nm, and the presence of metal−CO stretching frequencies is indicative of CpMn tricarbonyls versus dicarbonyls (Table S3, Supporting Information). This assignment is further supported by the formation of its derivatives including the facile photochemical conversion to the pyridine chelate **15** since it is well established that the side-chain functional groups rapidly coordinate manganese following irradiation of $CpMn(CO)_3$ derivatives.[4,5,12] The assignment of **15** is consistent with optical absorption above 400 nm (λ_{max} = 436 nm, shoulder = 490 nm) characteristic of the MLCT transitions responsible for the red-orange solutions typical of pyridine coordination like that in

Scheme 5

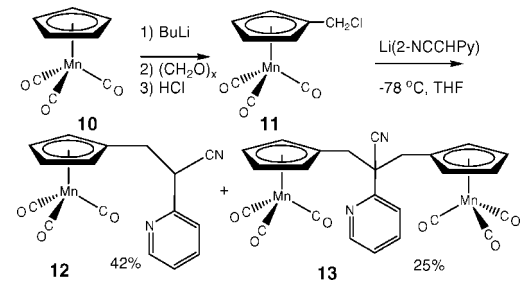

Scheme 6

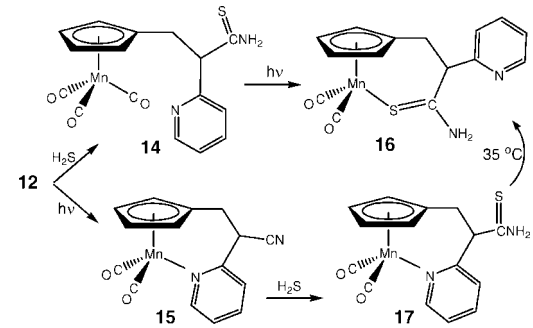

$CpMn(CO)_2$pyridine and **1**.[2,8] Chelation via the nitrile group is ruled out by previous studies demonstrating that manganese coordination of a cyclopentadienyl side-chain nitrile is unfavorable in a six-membered ring.[13] In fact, extended irradiation of pure **15** in methylcyclohexane-d_{14} at −50 °C with visible light did not lead to new NMR peaks. A substantial increase in the difference in chemical shifts for the diastereotopic methylene hydrogens in **15** versus **12** is also consistent with chelation where restricted rotation of the chelate ring enhances the differences in the chemical environments for the two hydrogens.

Reactions of the nitriles **15** and **12** with hydrogen sulfide and base resulted in high yields of thioamides **17** (72%) and **14** (95%), respectively. The assignments of the thioamides were consistent with the presence of NH peaks (9–11 ppm) in the proton NMR spectra. Like **15**, **17** shows a large difference in the diastereotopic methylene hydrogens in contrast to that observed for the corresponding unchelated **14**, an observation consistent with a methylene group in a chelate ring.

UV irradiation of a colorless solution of **14** in THF produced an orange solution (λ_{max} = 450 nm) with NMR peaks assigned to **16** (Table 1) with no evidence of **17**. The thioamide chelate **16** was identified by the large separation (1.3 ppm) of the *anti* and *syn* amide protons and the negligible change in the pyridine proton NMR peak positions relative to **14**. Like **15** and **17**, the large difference in the diastereotopic methylene hydrogens for **16** (compared to **14**) is consistent with the methylene group in a chelate ring for **16**. This assignment is also supported by the independent preparation of **16** via **17** where the thioamide group

(10) A reviewer noted the large difference in the calculation of the energy (6 kcal/mol for the gas phase) between **9** and **20** in Scheme 4. Previous studies indicate the structurally related 2-formylpyridine has an *s-trans* to *s-cis* free energy difference of 2 kcal/mol in solution and 7 kcal/mol in the gas phase.[11] Furthermore, the coordination of the carbonyl oxygen can be expected to polarize the carbonyl group, making the energy difference between the *s-trans* and *s-cis* conformers larger.

(11) For leading references see: Benassi, R.; Folli, U.; Schenetti, L.; Taddei, R. *J. Chem. Soc., Perkin Trans. 2* **1987**, 962–968.

(12) Yeh, P.-H.; Pang, Z.; Johnston, R. F. *J. Organomet. Chem.* **1996**, *509*, 123–129.

(13) Rybinskaya, M. I.; Korneva, L. M. *J. Organomet. Chem.* **1982**, *231*, 25–35.

was created after pyridine coordination. While attempting to isolate **17** during the evaporation of solvent at 35 °C, it isomerized to **16**. The facile isomerization of **17** (along with some likely initial photoisomerization) may explain the lack of observation of **17** following irradiation of **14**. This isomerization also demonstrates that **16** is more stable that **17**.

Linkage Isomerization of 16 and 17. Barring a conformational preference that always places the thioamide of **14** near the metal, we anticipated production of a mixture of thioamide (**16**) and pyridine (**17**) chelates upon irradiation of **14**. Instead, only **16** was observed (Scheme 6), and even irradiation of **16** with UV or visible light failed to produce new NMR peaks. This observation was unexpected considering **15** is thermally stable (as is $CpMn(CO)_2(pyridine)$[2,8]) and both **15** and **17** have identical chelate rings except for the nonchelated functional groups. Taken with the results for **7**−**9**, this observation suggests that **17** probably forms upon irradiation of **14** or **16**, but a relatively low-energy barrier leads to the isomerization of **17** faster than its formation.

Summary and Conclusions

We have prepared a tricarbonyl cyclopentadienyl manganese derivative with side-chain pyridine and ketone groups (**7**) that coordinates either group following photodissociation of a metal-carbonyl to form purple-red (**8**) and blue (**9**) chelates. The results demonstrate that **8** and **9** are a photochromic pair of isomers and irradiation of **8** results in a linkage isomerization to **9**, which isomerized thermally to **8**. We conclude that the side-chain ketone coordination is kinetically unstable relative to pyridine coordination and **9** isomerizes to **8** with an activation enthalpy and entropy of linkage isomerization of 21.4 kcal/mol and 3.5 eu, respectively. Furthermore, calculations and kinetic results indicate that a small stabilization of **9** or increase in the transition-state energy for isomerization (about 5 kcal/mol) could lead to a bistable, photochromic system. In contrast, light-driven linkage isomerization of **16** to **17** is not observed but likely occurs followed by a low-barrier thermal isomerization back to the more stable thioamide chelate. The results highlight the probability that facile η^1-N to η^2-arene linkage isomerization occurs for many stable pyridine chelates but is undetected without a stable isomer.

Experimental Section

Except where noted, chemicals were used as received from Aldrich, and procedures were carried out under argon or nitrogen atmosphere using a glovebox or standard Schlenk techniques. The argon for the Schlenk techniques was purified with an Ace-Burlitch inert atmosphere system (ACE Glass, Inc.). Ethanol (Aaper Alcohol and Chemical) was 200 proof ACS grade. Pyridine (from Mallinckrodt) was distilled after refluxing over calcium hydride or NaK under argon. Tricarbonyl{methyl(η^5-cyclopentadienyl)}manganese (**3**, Pressure Chemical) was distilled under vacuum (80 mTorr) at 54 °C. THF (Fisher), hexane, and heptane were distilled under argon after refluxing over NaK alloy. Tricarbonyl(η^5-cyclopentadienyl)-manganese was purchased from Strem or was a gift from Dr. John Sheats and was used as received.

Instrumentation. Spectra were obtained on a 270 MHz JEOL NMR spectrometer, a 500 MHz Varian NMR system, Mattson Galaxy 2020 FT-IR spectrometer, and Agilent 8453 UV–vis spectrophotometer. NMR assignments for **7** and **8** were supported by COSY, HMBC, and HMQC spectra. Chemical shifts were referenced to TMS in ppm using residual solvent peaks as internal standards. UV irradiation was supplied by a Rayonet photochemical reactor (RPR-100) equipped with 300 nm lamps (RPR-3000), a single 300 nm lamp reactor, or nitrogen lasers (PRA LN1000 or PTI GL3300). Visible irradiation at 60 cm was supplied by a 500 W quartz lamp (Commercial Electric L-38) with a water filter or a PTI dye laser with PLD500 dye.

Synthesis. Tricarbonyl[η^5-(2-(2-pyridinyl)ethyl)cyclopentadienyl]manganese(I), [Mn{η^5-$C_5H_4CH_2CO$(2-py)}$(CO)_3$], 6, and Tricarbonyl[η^5-(2-oxo-2-(2-pyridinyl)ethyl)cyclopentadienyl]manganese(I), [Mn{η^5-$C_5H_4CH_2CO$(2-py)}$(CO)_3$], 7. While **3** (4.0 g, 18.5 mmol), t-BuOK (2.2 g, 20 mmol), and dimethylformamide (10 mL) were stirred for 1 h the solution became red. After addition of **4** (3.8 mL, 39.8 mmol) the solution was stirred an additional hour and turned dark red. Water (2 mL) and 1 M HCl were added to until the solution was acidic. The solution was neutralized with $NaHCO_3$ and extracted with 100 mL of diethyl ether. The organic layer was dried with $MgSO_4$ and reduced by rotary evaporation. The residue was eluted on silica gel with ethyl acetate/hexane (5%). The first yellow band was **3** (1.5 g, 38%); the second yellow band was an orange solid (0.25 g) containing a mixture of several products (not characterized); the third yellow band gave a yellow-brown solid (**7**, 2.1 g, 34%), from which a diffraction-quality crystal was selected. Anal. Found (Calcd): C 55.64(55.75), H 3.39(3.12), N 4.26(4.33). ϵ_{281}(benzene) 6100 M^{-1} cm^{-1}, ϵ_{330}(benzene) 1800 M^{-1} cm^{-1}. H NMR (DMSO-d_6): δ 4.23 (s, 2H, CH_2), 4.91 (m, 2H, 3,4-Cp), 5.10 (m, 2,5-Cp), 7.72 (m, 1H, 5-py), 8.06 (m, 1H, 3-py), 8.08 (m, 1H, 4-py), 8.79 (m, 1H, 6-py). ^{13}C NMR (DMSO-d_6): δ 36.0 (CH_2), 82.7 (3,4-Cp), 85.2 (2,5-Cp), 99.1 (1-Cp), 121.6 (3-py), 128.0 (5-py), 137.7 (4-py), 149.2 (6-py), 152.0 (2-py), 197.3 (C═O), 225.5 (CO). The fourth yellow band gave a red-orange solid product (**5**, 0.9 g, 16%). ^{1}H NMR ($CDCl_3$): δ 4.74 (m, 2H, Cp), 5.07 (m, 2H, Cp), 6.82 (d, 1H *J* 15.8, CH), 7.13 (m, 2H, CH and Py), 7.26 (m, 1H, Py), 7.64 (m, 1H, Py), 8.55 (m, 1H, Py). ^{13}C NMR ($CDCl_3$): δ 82.4 (Cp), 99.0 (Cp), 122.2 (Py), 122.5 (CH), 125.0 (Py), 129.3 (CH), 136.7 (Py), 149.8 (Py), 154.6 (Py), 224.7 (CO).

Tricarbonyl(2-(2-pyridinyl)ethyl(η^5-cyclopentadienyl)manganese, [Mn{η^5-$C_5H_4CH_2CH_2$(2-py)}$(CO)_3$], 6. 5 (200 mg, 0.65 mmol), Pd/C (10%, 10 mg), and absolute ethanol (50 mL) were shaken for 12 h at 12 psi of H_2 using a Parr hydrogenator (model 3916EG). The resulting solution was filtered and concentrated by rotary evaporation to obtain a brown liquid. ^{1}H NMR ($CDCl_3$): δ 2.72 (m, 2H, CH_2), 2.96 (m, 2H, CH_2), 4.59 (m, 4H, Cp), 7.11 (m, 2H, C_5H_4N), 7.58 (m, 1H, C_5H_4N), 8.54 (m, 1H, C_5H_4N).

Dicarbonyl[2-oxo-2-(2-pyridinyl)-κN-ethyl(η^5-cyclopentadienyl]manganese, [Mn{η^5-$C_5H_4CH_2C$(O)(2-py-κN)}$(CO)_2$], 8. 7 (0.47 g, 1.4 mmol) in THF (200 mL) was irradiated 5 h with a 300 nm lamp under argon in an immersion-well photochemical reactor. The solvent was removed by trap-to-trap distillation to obtain a dark red solid (0.41 g, 93% yield). Anal. Found (Calcd): C 50.34(56.97), H 4.73(3.41), N 3.31(4.75). Crystals suitable for single-crystal diffractometry were grown from solutions of ether and hexanes at −78 °C. ϵ_{347}(benzene) 810 M^{-1} cm^{-1}, ϵ_{482}(benzene) 920 M^{-1} cm^{-1}. ^{1}H NMR (DMSO-d_6): δ 3.52 (s, 2H, CH_2), 3.85 (m, 2H, 3,4-Cp), 5.00 (m, 2,5-Cp), 7.21 (m, 1H, 5-py), 7.51 (m, 1H, 3-py), 7.81 (m, 1H, 4-py), 8.80 (m, 1H, 6-py). ^{13}C NMR (DMSO-d_6): δ 37.7 (CH_2), 78.4 (3,4-Cp), 81.3 (2,5-Cp), 96.3 (1-Cp), 125.4 (5-py), 126.3 (3-py), 137.3 (4-py), 159.1 (6-py), 159.3 (2-py) 193.9 (C═O), 234.7 (CO).

Tricarbonyl[hydroxymethyl(η^5-cyclopentadienyl]manganese, [Mn(η^5-$C_5H_4CH_2OH$)$(CO)_3$].[14] BuLi/pentane solution (11 mL, 2 M, 22 mmol) was added dropwise to **10** (4.0 g, 20 mmol) and THF (25 mL) and stirred at −78 °C for 2 h. A suspension of paraformaldehyde (1.8 g, 60 mmol) in THF (10 mL) was added dropwise, and after an additional stirring (4 h) the solution equilibrated to room temperature and was quenched with 5 mL of

(14) Herberhold, M.; Biersack, M. *J. Organomet. Chem.* **1995**, *503*, 277–287.

water. The organic layer was concentrated and eluted from silica with diethyl ether/hexane (40%). A second yellow band, after rotary evaporation, gave 3.7 g (81%) of yellow solid. ^{1}H NMR ($CDCl_3$): δ 1.62 (s, br, 1H, OH), 4.33 (s, br, 2H, CH_2), 4.70 (m, 2H, Cp), 4.82 (m, 2H, Cp). ^{13}C NMR ($CDCl_3$): δ 58.84 (CH_2), 82.11 (Cp), 82.24 (Cp), 104.85 (Cp), 224.65 (CO). Lit.:[14] δ 1.58 (t, 1H, OH), 4.32 (d, 2H, CH_2), 4.69 (s, broad, 2H, Cp), 4.80 (s, br, 2H, Cp). δ 58.8 (CH_2), 82.0 (Cp), 82.3 (Cp), 104.5 (Cp), 224.6 (CO).

Tricarbonyl[chloromethyl(η^5-cyclopentadienyl]manganese, [Mn(η^5-$C_5H_4CH_2Cl$)(CO)$_3$], 11. HCl was bubbled for 2 h through 10 mL of dichloromethane and tricarbonyl[hydroxymethyl-(η^5-cyclopentadienyl]manganese (4.1 g, 17.6 mmol) cooled to 0 °C. The solution was dried with Na_2SO_4, and the solvent was removed by rotary evaporation to yield a yellow solid, 4.10 g (93%). ^{1}H NMR (DMSO-d_6): δ 4.42 (s, 2H, CH_2), 4.99 (m, 2H, Cp), 5.24 (m, 2H, Cp). ^{13}C NMR (DMSO-d_6): δ 83.15 (CH_2), 83.78 (CH_2, Cp 3,4), 85.66 (CH_2, Cp 2,5), 101.60 (C, Cp 1), 225.44 (CO).

Tricarbonyl(2-cyano-2-(2-pyridinyl)ethyl(η^5-cyclopentadienyl)manganese, [Mn{η^5-$C_5H_4CH_2CH(CN)(2\text{-py})$}(CO)$_3$], 12, and [$\mu$-{1,1′-(2-cyano-2-(2-pyridinyl)propane-1,3-diyl)di(η^5-cyclopentadienyl)}]bis(tricarbonylmanganese),[Mn$_2${(η^5-$C_5H_4CH_2$)$_2$CH(CN)(2-py)}(CO)$_6$], 13. 2-Cyanomethylpyridine (2.20 g, 18.3 mmol) in THF (10 mL) was added to a 0 °C solution of NaH (0.37 g, 15.4 mmol) and THF (50 mL). After stirring for 4 h, **11** (3.8 g, 15 mmol in 15 mL of THF) was added dropwise. The solution was heated and stirred overnight at 55 °C and quenched with 3 mL of water, and the solvent was removed by using rotary evaporation. Two yellow bands were eluted from silica gel with 20% ethyl acetate/hexane. The second yellow band gave 2.10 g (42%) of a yellow viscous liquid. **12**: ^{1}H NMR (DMSO-d_6): δ 2.92 (m, 2H, CH_2), 4.60 (m, 1H, CH), 4.93 (m, 4H, Cp), 7.41 (m, 1H, 5-py), 7.43 (m, 1H, 3-py), 7.85 (m, 1H, 4-py), 8.60 (m, 1H, 6-py). The first yellow band yielded 2.05 g of a yellow powder (25%). **13**: A crystal structure has been reported.[15] ^{1}H NMR (DMSO-d_6): δ 3.08 (m, 4H, 2CH_2), 4.07 (m, 2H, 2Cp), 4.75 (m, 2H, 2Cp), 4.92 (m, 2H, 2Cp), 5.08 (m, 2H, 2Cp), 7.43 (m, 2H, C_5H_5N), 7.85 (m, 1H, C_5H_5N), 8.69 (m, 1H, C_5H_5N).

Tricarbonyl[2-carbothioamide-2-(2-pyridinyl)ethyl(η^5-cyclopentadienyl]manganese, [Mn{η^5-$C_5H_4CH_2CH(C(S)NH_2)(2\text{-py})$}(CO)$_3$], 14. 12 (0.95 g, 2.8 mmol), pyridine (1.5 mL), and triethylamine (0.5 mL) were bubbled for 12 h with H_2S. Hydrogen sulfide was prepared by adding HCl (10%) dropwise to $Na_2S \cdot 9H_2O$. Volatile components were removed by trap-to-trap distillation, and the residue was washed with two 10 mL portions of hexane to obtain 1.0 g of yellow powder (95%). Anal. Found (Calcd): C 52.37(52.18), H 3.89(3.56), N 7.45(7.61). ϵ_{281}(benzene) 9400 M^{-1} cm^{-1}, ϵ_{330}(benzene) 1100 M^{-1} cm^{-1}. ^{1}H NMR (DMSO-d_6): δ 3.04 (m, 2 H, CH_2), 4.24 (m, 1H, CH), 4.88 (m, 4H, Cp), 7.28 (m, 1H, C_5H_5N), 7.46 (m, 1H, C_5H_5N), 7.75 (m, 1H, C_5H_5N), 8.51 (m, 1H, C_5H_5N), 9.47 (s, br, 1H, NH_2), 9.61 (s, br, 1H, NH_2). ^{13}C NMR (DMSO-d_6): δ 32.55 (CH_2), 62.34 (CH), 82.98 (Cp), 83.28 (Cp), 84.45 (Cp), 105.00 (C_5H_5N), 123.13 (C_5H_5N), 137.20 (C_5H_5N), 149.25 (C_5H_5N), 159.01 (C_5H_5N), 206.82 (C═S), 226.20 (CO).

Dicarbonyl[2-cyano-2-(2-pyridinyl)-κN-ethyl(η^5-cyclopentadienyl]manganese, [Mn{η^5-$C_5H_4CH_2CH(CN)(2\text{-py}$-$\kappa N$}(CO)$_2$], 15. 12 (0.60 g, 1.8 mmol) and THF (200 mL) were irradiated for 18 h in a manner similar to the preparation of **8**. A red solution was obtained, and after solvent evaporation a red solid was washed with two 5 mL portions of ice-cold ethanol. The product was dried under vacuum to obtain 0.48 g (84% yield). ^{1}H NMR (C_6D_6): δ 1.39 (t, 1H, CH_2), 2.35 (m, 1H, CH_2), 2.85 (m 1H, Cp), 3.14 (m, 1H, CH), 3.92 (m 1H, Cp), 4.12 (m 1H, Cp), 4.41 (m 1H, Cp), 5.74 (m, 1H, C_5H_5N), 6.45 (m, 1H, C_5H_5N), 7.11 (under solvent peak), 9.01 (m, 1H, C_5H_5N).

Dicarbonyl[2-carbothioamide-κS-2-(2-pyridinyl)ethyl(η^5-cyclopentadienyl]manganese, [Mn{η^5-$C_5H_4CH_2CH(C(S)NH_2)$-κS-(2-py)}(CO)$_2$], 16. Method 1. 14 (390 mg, 1.06 mmol) and THF (200 mL) were irradiated for 6 h in a manner similar to the preparation of **8**. After trap-to-trap distillation, a red residue was eluted with 40% hexane/THF solution on silica plates. The red band was extracted with THF, the extract was filtered, and trap-to-trap distillation yielded 222 mg of red solid (62%).

Method 2. 15 (354 mg, 1.12 mmol), pyridine (3 mL), and triethylamine (3 mL) were bubbled with H_2S for 7 h. After trap-to-trap distillation a red residue was dried under vacuum for 24 h at 35 °C and then dissolved in THF (10 mL). Trap-to-trap distillation yielded 274 mg (72% yield). Anal. Found (Calcd): C 53.15(52.94), H 4.35(3.85), N 7.81(8.23). ϵ_{347}(benzene) 1580 M^{-1} cm^{-1}, ϵ_{482}(benzene) 4600 M^{-1} cm^{-1}. ^{1}H NMR (DMSO-d_6): δ 2.45 (m, 1H, CH_2), 3.18 (m, 1H, CH_2), 3.40 (m, 1H, Cp), 3.75 (m, 1H, Cp), 4.08 (m, 1H, Cp), 4.29 (m, 1H, CH), 4.60 (m, 1H, Cp), 7.31 (m, 1H, C_5H_5N), 7.33 (m, 1H, C_5H_5N), 7.80 (m, 1H, C_5H_5N), 8.63 (m, 1H, C_5H_5N), 9.17 (br, 1H, NH_2), 10.45 (br, 1H, NH_2).

Dicarbonyl[2-carbothioamide-2-(2-pyridinyl)-κN-ethyl(η^5-cyclopentadienyl]manganese, [Mn{η^5-$C_5H_4CH_2CH(C(S)NH_2)(2\text{-py}$-$\kappa N$}(CO)$_2$], 17. 15 (355 mg, 1.12 mmol), pyridine (3 mL), and triethylamine (3 mL) were bubbled with the hydrogen sulfide for 7 h. A red residue was obtained after trap-to-trap distillation and dried under vacuum (200 mTorr, 48 h) to yield 412 mg (88%). ^{1}H NMR (DMSO-d_6): δ 2.40 (m, 1H, CH_2, solvent overlap), 2.83 (m, 1H, CH_2), 3.30 (s, 1H, Cp), 3.92 (m, 1H, Cp), 4.15 (m, 1H, CH), 4.94 (m, 1H, Cp), 5.25 (m, 1H, Cp), 6.98 (m, 1H, C_5H_5N), 7.65 (m, 1H, C_5H_5N), 7.78 (m, 1H, C_5H_5N), 9.10 (m, 1H, C_5H_5N), 9.53 (m, 1H, NH_2), 10.00 (m, 1H, NH_2).

Single-Crystal Diffractometry. The single-crystal structure of **7** was determined using a Bruker model AXS Smart 1000 X-ray diffractometer equipped with a CCD area detector and a graphite, monochromatic Mo source (Kα = 0.71073 Å). The instrument was fitted with an upgraded Nicolet model LT-2 low-temperature controller. Crystals coated with paratone oil (Exxon) were mounted on a polymer loop under a nitrogen stream at −100 °C. Global refinement of unit cell, orientation matrix data, and data reductions were performed using SAINT 6.02.[21] Structure refinement was performed using the SHELXTL 5.1 and WinGX software packages.[16,17] The SADABS program was used to make empirical absorption corrections.[18] The structure of **8** was likewise determined except for the use of a Bruker AXS Proteum diffractometer with a CCD area detector and graphite-monochromated rotating anode Cu source (K =1.54178 Å). Data collection and global unit cell refinement for **8** was done using Proteum2 software.[19] ORTEP graphics were created using Raster3D.[20] Complete listings of atom coordinates, bond distances, angles, torsion angles, atomic displacement factors, and H atom coordinates may be found in the Supporting Information.

Irradiation Experiments. 8: For UV–vis spectra, 2 mL of an **8** stock solution (10 mg, 34 μmol in 25 mL of heptane) was diluted to 10 mL with heptane. The dilute solution (2.5 mL) was irradiated with visible light for four 20 s intervals in a cuvette at 25 °C. Spectra were obtained after each 20 s interval and then every 40 s (360 s total) without irradiation. For NMR spectra, **8** (3 mg, 10 μmol) and 1 mL of methylcyclohexane-d_{14} in a NMR tube was irradiated

(15) Duke, C. B.; To, T. T.; Ross, C. R.; Burkey, T. J. *Acta Crystallogr. E* **2007**, *E63*, m1848–m1849.

(16) Sheldrick, G. M. *A Program for the Refinement of Crystal Structures*; University of Gottingen: Gottingen, Germany, 1997.

(17) Farrugia, L. J. *J. Appl. Crystallogr.* **1999**, *32*, 837–838.

(18) Sheldrick, G. M. University of Gottingen: Gottingen, Germany, 1996.

(19) *Bruker PROTEUM2 Version 1.0*; Bruker AXS Inc.: Madison, WI, 2005.

(20) (a) ORTEP3 for Windows. Farrugia, L. J. *J. Appl. Crystallogr.* **1997**, *30*, 565. (b) Merritt, E. A.; Bacon, D. J. *Methods Enzymol.* **1997**, *277*, 505–524.

(21) Frisch, M. J. et al. *Gaussian 03, Revisions B.03 and B.05*; Gaussian, Inc.: Wallingford, CT, 2004.

with visible light for 5 min at −25 to −5 °C. Spectra were obtained at 5 °C and after warming the sample to 25 °C. The experiment was continued as irradiation and temperature changes were repeated twice more with this sample. For IR spectra, **8** (9.0 mg, 30 μmol) in 50 mL of heptane was irradiated with visible light in a NaCl cell (2 mm) for 1 min at 25 °C. A spectrum was recorded immediately and after 5 min of thermal equilibration. The experiment was continued as irradiation and temperature changes were repeated twice more.

15: For NMR spectra, **15** (3 mg, 10 μmol) in 1 mL of methylcyclohexane-d_{14} at −50 °C was irradiated 20 min with visible light. The sample was then transfer to an NMR probe cooled to −50 °C.

16: For NMR spectra, a solution of **16** (3 mg, 9 μmol) in 1 mL of benzene-d_6 was filtered and irradiated in an NMR tube at 450 nm for 90 min and at 400 nm for 30 min with the dye laser. The solution was irradiated further at 337 nm with a nitrogen laser for 30 min. A second sample of **16** in an NMR tube was irradiated with a 300 nm lamp for 8 min.

Acetophenone and **3**: Under an argon atmosphere, **3** (4 μL, 25 μmol) and acetophenone (15 μL, 129 μmol) were added to 1 mL of benzene-d_6 in an NMR tube. The sample was irradiated with UV light for 5 min.

Calculations. The theoretical calculations have been carried out using the Gaussian03[21] implementations of B3LYP [Becke three-parameter exchange functional (B3)[22] and the Lee–Yang–Parr correlation functional (LYP)[23]] and PBE [the PBE exchange functional and correlation functionals[24]] density functional theory[25] with the default pruned fine grids for energies (75, 302), default pruned coarse grids for gradients and Hessians (35, 110) [neither grid is pruned for manganese], and default SCF convergence for geometry optimizations (10^{-8}). All calculations used the same basis set combination. The basis set for manganese (341/341/41/1) was the Hay and Wadt basis set and effective core potential (ECP) combination (LanL2DZ)[26] as modified by Couty and Hall (341/341/41), where the two outermost p functions have been replaced by a (41) split of the optimized manganese 4p function,[27] supplemented with a single set of f polarization functions.[28] All carbons, oxygens, nitrogens, and hydrogens utilized the 6-31G(d′) basis set.[29,30] The density fitting approximation[31] for the fitting of the Coulomb potential was used for all PBE calculations; auxiliary density-fitting basis functions were generated automatically (by the procedure implemented in Gaussian 03) for the specified AO basis set. Spherical harmonic d and f functions were used throughout; that is, there are five angular basis functions per d function and seven angular basis functions per f function. All structures were fully optimized, and analytical frequency calculations were performed on all structures to ensure either a minimum or first-order saddle point was achieved. All reported energies are relative PBE energies. B3LYP optimized geometries and energies were quantitatively similar to those from PBE, and are not reported.

Acknowledgment. This study is based in part upon work supported by the National Science Foundation under grants CHE-0227475, -0353885, and -0443627 (T.J.B.). Early computational work in this study was supported at Texas A&M University by CHE 98-00184 and MRI 02-16275 and the Welch Foundation (Grant No. A-648), for which C.E.W. gratefully thanks Professor Michael B. Hall. Further computational work was performed on resources at the University of Memphis High-Performance Computing Facility. Stipend support was provided by the National Institute of Standards and Technology Grant 70NANB4H1093 (C.B.D.). Additional support of this research by the Cancer Center Support CORE Grant, P30 CA-21765, and the American Lebanese Syrian Associated Charities (ALSAC) is gratefully acknowledged by C.R.R.

Supporting Information Available: Additional NMR and IR spectroscopic data, photochemical experiments with **7**, a summary of X-ray crystallographic data, and CIF files for **7** and **8**; further computational results for higher energy pathways. This material is available free of charge via the Internet at http://pubs.acs.org.

OM701101H

(22) Becke, A. D. *J. Chem. Phys.* **1993**, *98*, 5648–5652.
(23) Lee, C.; Yang, W.; Parr, R. G. *Phys. Rev. B* **1988**, *37*, 785–789.
(24) (a) Perdew, J. P.; Burke, K.; Ernzerhof, M. *Phys. Rev. Lett.* **1996**, *77*, 3865–3868. (b) Erratum: *Phys. Rev. Lett.* **1997**, *78*, 1396.
(25) Parr, R. G.; Yang, W. *Density Functional Theory of Atoms and Molecules*; Oxford University Press: New York, 1989.
(26) (a) Hay, P. J.; Wadt, W. R. *J. Chem. Phys.* **1985**, *82*, 270–283. (b) Wadt, W. R.; Hay, P. J. *J. Chem. Phys.* **1985**, *82*, 284–298.
(27) Couty, M.; Hall, M. B. *J. Comput. Chem.* **1996**, *17*, 1359–1370.
(28) Ehlers, A. W.; Böhme, M.; Dapprich, S.; Gobbi, A.; Höllwarth, A.; Jonas, V.; Köhler, K. F.; Stegmann, R.; Veldkamp, A.; Frenking, G. *Chem. Phys. Lett.* **1993**, *208*, 111–114.
(29) Hariharan, P. C.; Pople, J. A. *Theor. Chim. Acta* **1973**, *28*, 213–222.
(30) The 6-31G(d′) basis set has the exponent for the d polarization function for C, O, and N taken from the 6-311G(d) basis sets, instead of the original arbitrarily assigned value of 0.8 used in the 6-31G(d) basis sets.
(31) (a) Dunlap, B. I.; Connolly, J. W. D.; Sabin, J. R. *J. Chem. Phys.* **1979**, *71*, 3396–3402. (b) Dunlap, B. I.; Connolly, J. W. D.; Sabin, J. R. *J. Chem. Phys.* **1979**, *71*, 4993–4999. (c) Dunlap, B. I. *J. Chem. Phys.* **1983**, *78*, 3140–3142. (d) Dunlap, B. I. *J. Mol. Struct. (Theochem)* **2000**, *529*, 37–40.